Superconducting proximity effect in Pb/Ag nanocomposites

Sangita Bose and Pushan Ayyub*
Department of Condensed Matter Physics and Material Science, Tata Institute of Fundamental Research, Mumbai 400005, India
(Received 30 January 2007; revised manuscript received 21 July 2007; published 23 October 2007)

We show that the superconducting transition temperature (T_C) of a two-component system consisting of a random distribution of Pb and Ag nanoparticles, with sizes less than their respective coherence lengths, is governed essentially by proximity effect. The microstructure of the nanodispersed two-phase system has been studied using in-lens secondary electron and energy selective backscattered electron detectors. The theory of the superconducting proximity effect as previously applied to bilayers and multilayers can be suitably modified to include the ratio of the volume fraction of the superconducting and the normal metal components so as to explain the observed variation in T_C in such nanocomposites with varying metal composition. Interestingly, Pb behaves as a weak-coupling superconductor in the random Pb-Ag nanocomposite.

DOI: 10.1103/PhysRevB.76.144510 PACS number(s): 74.45.+c, 74.78.Na, 81.07.Bc, 61.46.Df

INTRODUCTION

When a superconductor is in close proximity with a normal metal or another superconductor with a lower transition temperature, the Andreev reflection leads to a leakage of Cooper pairs into the normal metal, while unpaired electrons from the normal metal diffuse into the superconductor. This leads to superconductivity being weakened in the superconductor and induced in the normal metal. The usual result is a lowering of the effective transition temperature (T_C) of the composite system. This phenomenon, known as the superconducting proximity effect (SPE), has been studied experimentally[1–6] and theoretically[7–10] in bilayers and alternating multilayers of many superconductor and normal metal combinations. The variation of the effective T_C of such systems has been studied as a function of the thickness of the individual superconducting and normal metal layers and the bilayer periodicity. The theory of SPE has been worked out for bilayers and multilayers in the weak-coupling limit (electron-phonon coupling constant for the superconductor, $\lambda < 1$) by De Gennes[7] and Werthamer[9] and in the strong-coupling limit ($\lambda > 1$) by Silvert.[10] An essential criterion for observing proximity effect is that the thickness of the individual components in the bilayer or multilayer should be less than their respective coherence lengths: $\xi_{N,S} = [\hbar D_{N,S}/2\pi k_B T]^{1/2}$, where $D_{N,S}$ is the diffusivity of the normal (superconducting) layer. Physically, ξ_S is the distance up to which the pair breaking effect of the Cooper pairs is felt in the superconductor across the S/N interface, and ξ_N is the distance within the normal metal up to which the superconducting pairing wave function penetrates. This is known as the "Cooper limit."[8] The value of $\xi_{S,N}$ for typical elemental superconductors usually ranges from 10 to 100 nm. Thus, the consequences of superconducting proximity can actually be observed in very thin layers.

Our understanding of nanometer scale superconducting particles embedded in a metallic (normal or superconducting) matrix, however, is much more limited. In such cases, besides the constraint of size, the matrix also controls the superconducting transition through SPE. Recently, Sternfeld *et al.*[11] have shown that in a random distribution of superconductor and normal metal nanoparticles, in which the grain size of each phase is less than the corresponding coherence length ($\xi_{S,N}$), one may replace the ratio of the thicknesses of the superconductor and normal metal layers (d_S/d_N) in the de Gennes–Werthamer theory[7,9] by the ratio of the volume fraction of the two components. Such an approach leads to a correct explanation of the dependence of T_C on the volume fraction of the two components in the nanocomposite system.

As there is very little work on such random two-phase nanocomposites, it is important to study their properties in greater detail and investigate the generality of the above conceptual approach in different systems. We have carried out a detailed study of the superconducting properties of a Pb-Ag nanocomposite (deposited in the form of a thin film) with varying composition. Note that Pb is a strong-coupling superconductor (with $T_C = 7.2$ K, $2\Delta/kT_C \sim 4.5$), while Ag remains normal down to very low temperatures. We show that the effective T_C of the Pb-Ag nanocomposites decreases monotonically from the bulk value (for pure Pb) with the decreasing volume fraction of Pb. Such a decrease cannot be attributed to finite size effects that have been earlier observed in elemental nanocrystalline superconductors.[12,13] The observed variation in T_C with the volume concentration of Pb can be correctly explained by the theory of the SPE valid for bilayers and multilayers, provided the ratio of the thickness of the two components is substituted by the ratio of the volume fraction of the two constituents in the nanocomposite. We also observe that Pb behaves as a weak-coupling superconductor when randomly dispersed in a normal metal with a slightly repulsive electron-phonon coupling interaction.

EXPERIMENT

Sputter deposition at relatively high pressures ($\sim$20–200 mTorr) and low substrate temperatures ($\sim$100–300 K) is known to produce nanocrystalline films.[14] The average particle size can be controlled by proper choice of sputtering voltage, gas pressure, and substrate temperature. In the present case, cosputtering from a composite Pb-Ag target was carried out using an axial, planar magnetron sputtering gun. The composite target was prepared by placing small pieces ($\sim 10 \times 5 \times 2$ mm^3) of Ag (99.99% pure) along an annular ring coinciding with the sputter zone

TABLE I. Sputter deposition conditions for the Pb:Ag nanocomposite samples.

Sample	Base pressure (Torr)	Ar pressure (mbar)	Voltage (V)	Current (mA)	Deposition time (min)
PbAg01	1.2×10^{-5}	0.027	260	30	5
PbAg12	5×10^{-6}	0.180	230	55	5
PbAg16	8.8×10^{-6}	0.250	235	35	10
PbAg14	4.5×10^{-6}	0.260	220	40	10
PbAg06	4.3×10^{-6}	0.270	270	100	10
PbAg05	5×10^{-6}	0.089	300	100	10
PbAg10	3.5×10^{-6}	0.130	280	60	10
PbAg07	4.2×10^{-6}	0.260	260	80	10
PbAg02	4×10^{-6}	0.059	300	45	5
PbAg03	5×10^{-6}	0.066	340	50	5
PbAg04	4.5×10^{-6}	0.026	340	54	10

on a commercial Pb target (5 cm diameter, 3 mm thick, from Kurt and Lesker Co., 99.999% pure). The composition (Pb/Ag ratio) for the nanocomposite films was altered by changing the target composition, while the grain sizes for the Pb and Ag phases were controlled *via* the sputtering conditions, as listed in Table I. In all cases, *p*-type Si (100) wafers were used as substrate. It is important to point out that even heavily doped Si does not produce any proximity effect when in contact with superconductors such as Nb.[15] In an independent study of nanostructured Pb films (with particle size down to ≈10 nm) grown on Si substrates, we found no change in T_C from the bulk value of 7.2 K.

The grain size (D) was determined in terms of the coherently diffracting domain size from x-ray diffraction (XRD) line broadening using the Scherrer formula after correcting for instrumental broadening. The grain sizes were approximately in the 20–60 nm range for Pb (D_{Pb}) and in the 7–25 nm range for Ag (D_{Ag}). The surface morphology and the elemental composition were obtained using a Zeiss Ultra 55 field emission scanning electron microscope (FE-SEM) based on a Gemini lens and a JEOL JSM-840 scanning electron microscope (SEM), both equipped with energy dispersive x-ray (EDX) analyzers. The elemental composition (from EDX) of the different nancomposite Pb-Ag films was in the range from Pb(9%)-Ag(91%) to Pb(100%), as listed in Table II. Elemental mapping showed a uniform distribution of Pb and Ag in all samples.

TABLE II. List of samples studied with their composition (obtained from EDAX), volume fraction (P_S/P_N), T_C, and x-ray domain size.

Sample	Atomic ratio (Pb:Ag)	P_S/P_N	T_C (K)	Particle size of Pb (nm)	Particle size of Ag (nm)
PbAg01	100:0	100	7.25	50	No XRD line
PbAg12	93:7	23.68	7.0	39	No XRD line
PbAg16	86:14	10.95	6.7	27	No XRD line
PbAg14	84:16	9.35	6.6	21	No XRD line
PbAg06	81:19	7.59	6.4	45	No XRD line
PbAg05	75:25	5.34	6.1	21	5.4
PbAg10	67:33	3.62	5.4	56	11
PbAg07	64:36	3.16	5.2	23	7
PbAg02	63:37	3.04	5.1	26	19
PbAg03	16:84	0.33	⋯	18	11
PbAg04	9:91	0.18	⋯	No XRD line	6

The superconducting T_C of the nanocomposite films was measured by the planar coil ac susceptibility technique. In this method, the thin film sample is sandwiched between two planar coils with the secondary coil picking up the signal induced by a current in the primary. When the sample becomes superconducting, the secondary signal is shielded by the sample as it goes into the Meissner state. Hence, a sharp drop in the signal is observed as the sample is cooled below T_C. Though it does not provide the absolute value of the diamagnetic moment, this is a very sensitive technique to determine the superconducting properties of thin films in which the volume of the superconducting component is very small. In conventional methods for magnetization measurement, the signal is proportional to the effective sample volume, while in the planar coil method, it basically depends on the area covered by the superconducting phase in between the two coils. The temperature at which the real part of the susceptibility (χ') deviated from zero was identified as T_C. Independent measurements show that this temperature matches closely with that at which the electrical resistivity vanishes and a macroscopic critical current density (J_C) can be sustained in the sample.

RESULTS AND DISCUSSIONS

A typical, low-resolution SEM image of a sample with 63 at. % Pb was obtained with the help of a Zeiss Ultra 55 FE-SEM, using an in-lens secondary electron (SEI) detector [Fig. 1(a)]. The image shows uniform microstructure with a narrow grain size distribution. However, this image does not allow one to distinguish between Pb and Ag grains. A compositional image of the nanoscale two-phase dispersion was successfully obtained using an energy selective backscatter (ESB) detector, also operated at a relatively low voltage (~1.8 kV). Figure 1(b) shows an ESB image of the same region, as Fig. 1(a), but the Pb and Ag particles here display different contrasts. It is clear that the lighter colored Pb particles are intimately mixed with the Ag particles, which have much darker contrast and are virtually invisible. Similar SEM images (but at higher magnification) of the sample with 81 at. % Pb are shown in Fig. 2. As before, Fig. 2(b) is an ESB image showing elemental contrast. It is apparent from Figs. 1(a) and 2(a) that the nanoparticles are largely aggregated into small clusters. However, the primary particles (that form the aggregates) have a reasonably uniform size distribution. Particle size distributions for two representative nanocomposite thin film samples obtained from high-resolution SEM images using standard image analysis packages are shown in Fig. 3. Note that these size distributions

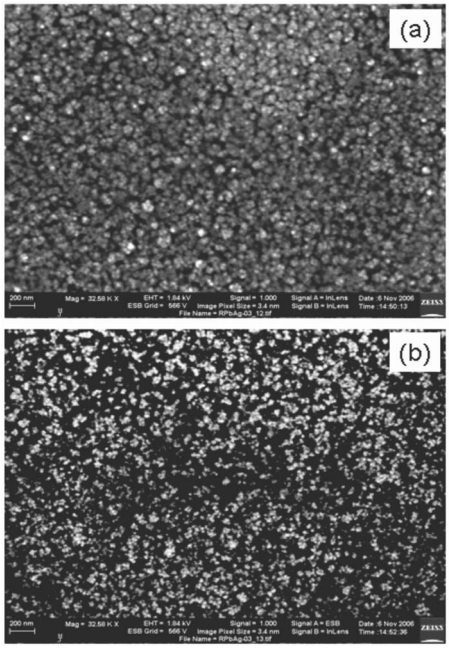

FIG. 1. SEM image (×32 500) of a Pb-Ag nanocomposite sample with 63 at. % Pb, showing perfectly uniform microstructure, obtained using (a) a normal (in-lens) secondary electron (SEI) detector and (b) an energy selective backscatter (ESB) detector. The (b) ESB image shows *only* the Pb nanoparticles.

were obtained from the ESB data and hence refer to the Pb nanoparticles only. The Ag nanoparticles have substantially smaller mean size in all cases. The mean crystallite sizes for the Pb and Ag nanoparticles were individually obtained (see Table II) from XRD line profile analysis using the WINFIT

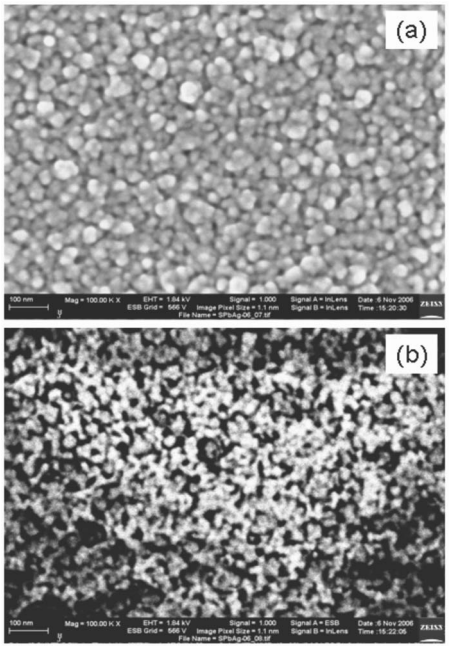

FIG. 2. SEM image (×100 000) of a Pb-Ag nanocomposite sample with 81 at. % Pb, obtained using (a) an SEI detector and (b) an ESB detector. As before, (b) shows only the Pb nanoparticles.

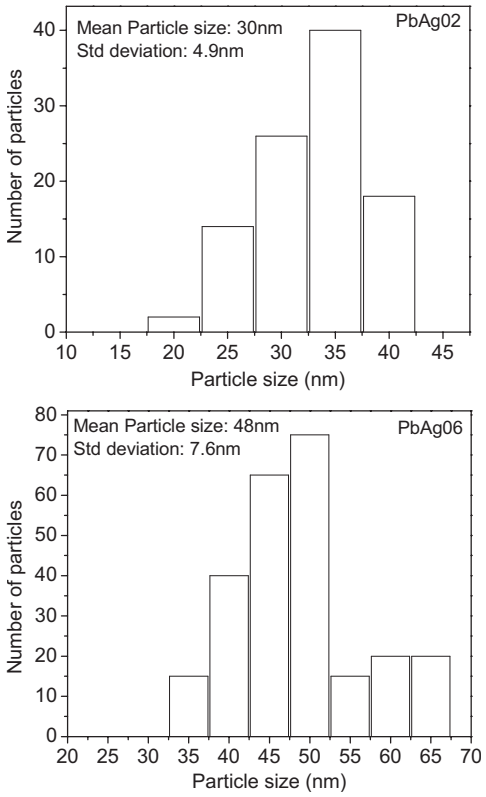

FIG. 3. Particle size distribution obtained from high-resolution SEM images for two representative nanocomposite samples, with 63 at. % Pb (top) and 81 at. % Pb (bottom). The standard deviation is typically about 15% of the mean size.

software. A comparison of Fig. 3 and Table II shows that the coherently diffracting x-ray domain size matches quite well with the mean primary particle size obtained from SEM.

We now present the superconducting properties of the Pb-Ag nanocomposite system. Figure 4 shows the temperature dependence of the real part of the ac susceptibility (χ') measured by the planar coil technique for nanocomposite samples with different compositions. There was a monotonic decrease in T_C (as obtained from the χ'-T data) from the bulk value of 7.25 to 5.1 K in the nanocomposite films as the at. % of Pb changed from 100 to 63. Films with less than

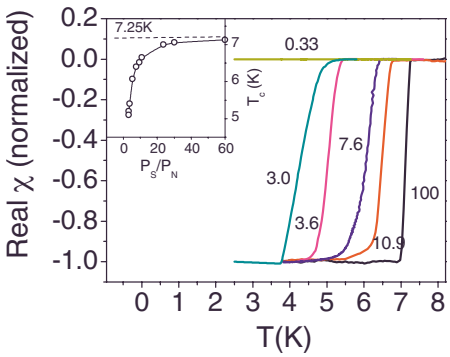

FIG. 4. (Color online) Temperature dependence of the real part of the ac susceptibility for the Pb-Ag nanocomposites with varying P_S/P_N ratio (indicated in figure). The inset shows the variation of T_C with the P_S/P_N ratio in the nanocomposite samples.

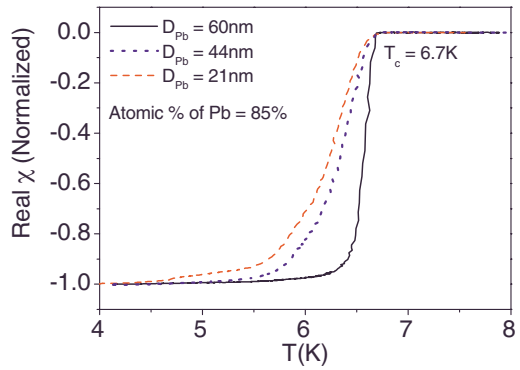

FIG. 5. (Color online) Temperature dependence of the real part of the ac susceptibility for the Pb-Ag nanocomposites with the same Pb/Ag ratio but different grain sizes.

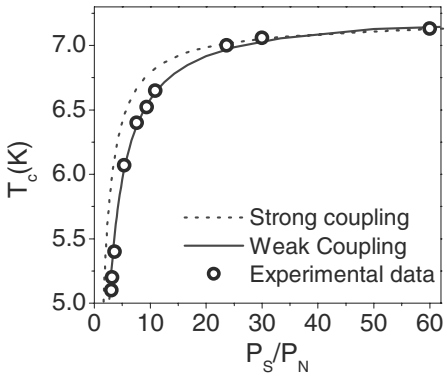

FIG. 6. Variation of T_C with the ratio of the volume fractions of Pb (P_S) and Ag (P_N). The accuracy of measuring either T_C or P_S/P_N is not larger than the size of the data points, shown by the open circles. The theoretical curves for the strong- and weak-coupling limits are shown by the dotted and solid lines, respectively.

20% of Pb were nonsuperconducting. The inset (Fig. 4) shows the decrease of T_C with decreasing volume fraction of Pb.

Since T_C (as well as other superconducting properties) also depends on the particle size of the superconductor, it is important to isolate proximity effect from particle size effects. To investigate the effect of particle size of Pb on T_C in the nonocomposites, we synthesized three samples with different grain sizes (D_{Pb}) in the 20–60 nm range but with nominally similar Pb/Ag ratio. Figure 5 shows the susceptibility data for three samples with different sizes but with ≈85 at. % Pb. It is clear that T_C remains roughly constant at ≈6.7 K, independent of the particle size. In a separate study[16] of particle size effects in pure nanocrystalline Pb, we found that T_C does not change down to a size of ≈10 nm, in conformity with existing data.[12,17] We therefore conclude that T_C of the nanocomposite films is dictated primarily by the ratio of the two components provided that the particle sizes of Pb and Ag are less than their respective coherence lengths, but larger than ≈10 nm. Expectedly, we also found that if the particle size of Pb is greater than 80 nm (coherence length of pure Pb), the corresponding T_C is the same as that of bulk Pb (≈7.2 K), since the SPE is not important in this size regime.

To understand our observations on the variation of T_C with the volume fraction of the superconducting and normal components, we adopt an approach similar to that of Sternfeld *et al.*[11] for the case of Pb-Cu. Following this approach, we substitute the ratio of the thickness of the superconductor and the normal metal in the SPE formalism for bilayers and multilayers by the ratio of the volume fractions of the two components in the nanocomposite system (say, P_S and P_N). Thus, the expression for T_C is

$$\ln\left(\frac{T_C}{1.14\Theta_D}\right) = \frac{1+\alpha(P_N/P_S)}{N_S(0)V}, \tag{1}$$

in the weak-coupling limit ($\lambda < 1$), where Θ_D is the Debye temperature, and

$$\ln(1.45T_C) = \frac{\lambda_S \ln \Theta_S + \lambda_N \ln \Theta_N \alpha(P_N/P_S)}{\lambda_S + \lambda_N \alpha(P_N/P_S)} - \frac{\lambda_S + 1 + (\lambda_N + 1)\alpha(P_N/P_S)}{\lambda_S - \mu + (\lambda_N - \mu)\alpha(P_N/P_S)}, \tag{2}$$

in the strong-coupling limit ($\lambda > 1$). Here, $\alpha = N_N(0)/N_S(0)$, where $N_N(0)$ and $N_S(0)$ are the density of states at the Fermi energy for the normal metal and the superconductor, respectively, while λ_N, Θ_N, λ_S, and Θ_S are the electron-phonon coupling constants and the Debye temperatures of the normal metal and the superconductor, respectively. V is the interelectron attractive potential due to phononic interaction and μ is the effective electron-electron repulsion term.

Theoretical curves for the strong- and weak-coupling limits were calculated using the following parameters from literature:[5,11] $\Theta_{\mathrm{Pb}} = 105$ K, $\Theta_{\mathrm{Ag}} = 215$ K, $\mu = 0.11$, $N_{\mathrm{Pb}}(0) = 0.276N_0$, $N_{\mathrm{Ag}}(0) = 0.098N_0$, $\lambda_{\mathrm{Pb}} = 1.013$, and $\lambda_{\mathrm{Ag}} = -0.018$, where N_0 is the Avogadro number. The value of $N_{\mathrm{Pb}}(0)V = 0.355$ was obtained from the weak-coupling BCS expression:[18] $T_C = 1.14\Theta \exp(-1/N(0)V)$ and taking T_C (Pb) = 7.25 K. λ_{Ag} is taken from the work of Kouh and Valles,[19] who studied SPE in quench condensed Pb/Ag bilayers. Their data on the variation of T_C with bilayer thickness could be fitted to SPE theory only if the electron-phonon coupling for Ag was taken to be slightly repulsive.

Figure 6 depicts our experimental data points and the calculated curves for the weak- and strong-coupling limits, shown, respectively, as a solid line and a dotted line. Though Pb is a well-known strong-coupling superconductor with $\lambda > 1$, our data fit better with the theoretical curve for the weak-coupling case. Thus, in such random mixtures of Pb and Ag nanoparticles, the slightly repulsive electron-phonon interaction in Ag appears to influence the interaction of the superconducting electrons with the lattice in the Pb nanoparticles. Such weak-coupling behavior of Pb has not been observed in bilayers or multilayers of Pb with normal metals. On the contrary, for pure nanocrystalline Pb, there are reports

showing that Pb tends to exhibit *stronger*-coupling behavior with decreasing grain size.[12]

In summary, we have shown that the superconducting T_C in a cosputtered, randomly intermixed composite of Pb and Ag nanoparticles is controlled by the ratio of the volume fraction of the two components, in accordance with the predictions of proximity effect. The exact nature of the nanoparticle dispersion has been shown from high-resolution electron microscopy data. The particle sizes corresponding to each phase should be smaller than the relevant coherence length for proximity effect to be observable. Quantum size effects due to the discretization of the energy bands are not important above $\approx$10 nm. We further show that Pb behaves as a weak-coupling superconductor when randomly distributed with a normal metal such as Ag.

ACKNOWLEDGMENTS

It is a pleasure to thank Heinrich Jaksch (Carl Zeiss SMT) for his help with the SEM images, Pratap Raychaudhuri for providing access to the susceptibility apparatus, and Raju Raychaudhuri for helping with the synthesis.

*pushan@tifr.res.in

[1] P. Hilsch, Z. Phys. **167**, 511 (1962).
[2] J. J. Hauser, H. C. Theurer, and N. Werthamer, Phys. Rev. **142**, 118 (1966).
[3] C. J. Kircher, Phys. Rev. **168**, 437 (1968).
[4] T. T. Chen and L. L. Kiang, Chin. J. Phys. (Taipei) **12**, 53 (1974).
[5] O. Bourgeois, A. Frydman, and R. C. Dynes, Phys. Rev. B **68**, 092509 (2003).
[6] R. Banerjee, P. Vasa, G. B. Thompson, H. L. Fraser, and P. Ayyub, Solid State Commun. **127**, 349 (2003).
[7] P. G. De Gennes, Rev. Mod. Phys. **36**, 225 (1964).
[8] L. Cooper, Phys. Rev. Lett. **6**, 689 (1961).
[9] N. R. Werthamer, Phys. Rev. **132**, 2440 (1963).
[10] W. Silvert, Phys. Rev. B **12**, 4870 (1975).
[11] I. Sternfeld, V. Shelukhin, A. Tsukernik, M. Karpovski, A. Gerber, and A. Palevski, Phys. Rev. B **71**, 064515 (2005).
[12] W. H. Li, C. C. Yang, F. C. Tsao, and K. C. Lee, Phys. Rev. B **68**, 184507 (2003).
[13] S. Bose, P. Raychaudhuri, R. Banerjee, P. Vasa, and P. Ayyub, Phys. Rev. Lett. **95**, 147003 (2005).
[14] P. Ayyub, R. Chandra, P. Taneja, A. K. Sharma, and R. Pinto, Appl. Phys. A **73**, 67 (2001).
[15] W. M. van Huffelen, T. M. Klapwijk, and E. P. T. M. Suurmeijer, Phys. Rev. B **47**, 5151 (1993).
[16] S. Bose, P. Raychaudhuri, and P. Ayyub (unpublished).
[17] S. Reich, G. Leitus, R. Popovitz-Biro, and M. Schechter, Phys. Rev. Lett. **91**, 147001 (2003).
[18] M. Tinkham, *Introduction to Superconductivity*, 2nd ed. (McGraw-Hill, Singapore, 1996), p. 63.
[19] T. Kouh and J. M. Valles, Jr., Phys. Rev. B **67**, 140506(R) (2003).